DALTON
FULL PAPER

p-Substituent effects on the redox chemistry of the diaryltriazenido-bridged dirhodium complexes $[Rh_2(CO)_{4-n}(PPh_3)_n(\mu\text{-}p\text{-}XC_6H_4NNNC_6H_4X'\text{-}p)_2]$ (n = 0–2)

Neil G. Connelly,[a] Paul R. G. Davis,[a] Emma E. Harry,[a] Phimphaka Klangsinsirikul[a] and Monika Venter[b]

[a] *School of Chemistry, University of Bristol, Bristol, UK BS8 1TS*
[b] *Department of Inorganic Chemistry, Babes-Bolyai University, Arany Janos 11, RO-3400, Cluj-Napoca, Romania*

Received 12th April 2000, Accepted 9th June 2000
Published on the Web 30th June 2000

The complexes $[Rh_2(CO)_4(\mu\text{-}p\text{-}XC_6H_4NNNC_6H_4X'\text{-}p)_2]$ (X = X′ = H, Me, Et, OMe, CN, F, Cl or Br; X = H, X′ = OMe or NO_2) were prepared in a two-step reaction involving the cleavage of $[\{Rh(\mu\text{-}Cl)(CO)_2\}_2]$ with the diaryltriazene $p\text{-}XC_6H_4NNNHC_6H_4X'\text{-}p$ followed by the deprotonation of the resulting mononuclear triazene complex $[RhCl(CO)_2\{N(C_6H_4X\text{-}p)NNHC_6H_4X'\text{-}p\}]$ with NEt_3. Yields of the dimeric products were maximised by carefully controlling the reaction time for each step. Reaction of the tetracarbonyls with PPh_3 gave the mono- and di-substituted species $[Rh_2(CO)_{4-n}(PPh_3)_n(\mu\text{-}p\text{-}XC_6H_4NNNC_6H_4X'\text{-}p)_2]$ (n = 1 or 2), the reaction times again depending on the substituents X and X′. Each binuclear complex undergoes at least one reversible one-electron oxidation reaction at a platinum electrode in CH_2Cl_2. In some cases, *e.g.* X = X′ = OMe, as many as three oxidation waves are observed; for X = H, X′ = NO_2, n = 1 or 2, well-defined reduction waves are apparent. The oxidation potential depends on the extent of carbonyl substitution (for each incremental increase in n the potential is decreased by *ca.* 300 mV) and on the triazenide ligand substituent such that $E^{\circ\prime}$ for the first oxidation wave can be varied systematically over a range of 800 mV. There is a linear relationship between $E^{\circ\prime}$ for the first oxidation step and the Hammett parameter σ_p but a poorer correlation for the second oxidation process.

Introduction

By means of the systematic carbonyl substitution reactions of the diaryltriazenide-bridged $[Rh_2]^{2+}$ complex $[Rh_2(CO)_4(\mu\text{-}p\text{-}XC_6H_4NNNC_6H_4X'\text{-}p)_2]$ we have stabilised the core oxidation levels $[Rh_2]^{3+}$ (*e.g.* in $[Rh_2(CO)_2(PPh_3)_2(\mu\text{-}p\text{-}XC_6H_4NNNC_6H_4X'\text{-}p)_2]^+$)[1] and $[Rh_2]^{4+}$ {*e.g.* in $[Rh_2Cl(CO)_2(bipy)(\mu\text{-}p\text{-}XC_6H_4NNNC_6H_4X'\text{-}p)_2]^+$ (bipy = 2,2′-bipyridine)}.[2] Throughout such studies[3] we have exclusively used the di-*p*-tolyltriazenide ligand ($p\text{-}XC_6H_4NNNC_6H_4X'\text{-}p$, X = X′ = Me), reasoning that the *p*-substituents X and X′ were unlikely to affect significantly the electron transfer properties; detailed structural studies, EPR spectroscopy and EHMO calculations had shown the HOMO of the $[Rh_2]^{2+}$ complexes to be an out of phase combination of the $4d_{z^2}$ orbitals on the two Rh atoms.[4] Recently, however, Ren has shown[5] that the *p*-substituents X and X′ do markedly affect the redox behaviour of diarylformamidinate complexes such as $[M_2\{\mu\text{-}p\text{-}XC_6H_4NC(H)NC_6H_4X'\text{-}p\}_4]$ (M = Ni,[6] Mo[7] and Rh[8]) and $[Ru_2\{\mu\text{-}p\text{-}XC_6H_4NC(H)NC_6H_4X'\text{-}p\}_4X_n]$ (X = C_2Ph, n = 2;[9] X = Cl, n = 1[10]). Given the extensive chemistry based on the electron-transfer reactions of $[Rh_2(CO)_4(\mu\text{-}p\text{-}MeC_6H_4NNNC_6H_4Me\text{-}p)_2]$, the attraction of being able to tune redox potentials further, and therefore reactivity, led us to investigate the effects of X and X′. We now report studies of the oxidation of $[Rh_2(CO)_{4-n}(PPh_3)_n(\mu\text{-}p\text{-}XC_6H_4NNNC_6H_4X'\text{-}p)_2]$ (X = X′ = H, Me, Et, OMe, CN, F, Cl or Br; X = H, X′ = OMe or NO_2; n = 0–2), three series of complexes which undergo one-electron oxidation with a marked dependence on X and X′ of oxidation potential, $E^{\circ\prime}$, quantified in terms of the Hammett σ_p parameter.[11] Other substituent effects are also observed. For example, for X = X′ = OMe as many as three oxidation waves are observed, and for X = H, X′ = NO_2, n = 1 or 2, well-defined reduction waves are apparent.

Results and discussion

The complexes $[Rh_2(CO)_4(\mu\text{-}p\text{-}XC_6H_4NNNC_6H_4X'\text{-}p)_2]$ (X = X′ = H, Me,[1] Et, OMe, CN, F, Cl or Br: X = H, X′ = OMe or NO_2) were prepared in two steps, namely (i) the reaction of $[\{Rh(\mu\text{-}Cl)(CO)_2\}_2]$ with the diaryltriazene $p\text{-}XC_6H_4NNNHC_6H_4X'\text{-}p$, and (ii) the reaction of the resulting mononuclear triazene complex $[RhCl(CO)_2\{N(C_6H_4X\text{-}p)NNHC_6H_4X'\text{-}p\}]$ with NEt_3 (Scheme 1). The yield of the binuclear tetracarbonyl $[Rh_2(CO)_4(\mu\text{-}p\text{-}XC_6H_4NNNC_6H_4X'\text{-}p)_2]$ from the second step is very dependent on the efficient formation of $[RhCl(CO)_2\{N(C_6H_4X\text{-}p)NNHC_6H_4X'\text{-}p\}]$ in the first. This in turn depends critically on X and X′ such that the rate of reaction between dimeric $[\{Rh(\mu\text{-}Cl)(CO)_2\}_2]$ and $p\text{-}XC_6H_4NNNHC_6H_4X'\text{-}p$ is fastest when the substituent is electron-donating; the reaction takes *ca.* 3 min for X = X′ = MeO but *ca.* 1 h for X = X′ = CN. However, where the cleavage reaction is rapid a further process, which gives uncharacterised products which do not yield the dimer on deprotonation, is observed. Thus, for maximum yields of the desired dimeric tetracarbonyl the formation of the mononuclear triazene complex was monitored carefully by IR spectroscopy.

Once purified, generally by column chromatography, the tetracarbonyls $[Rh_2(CO)_4(\mu\text{-}p\text{-}XC_6H_4NNNC_6H_4X'\text{-}p)_2]$ (X = X′ = H, Me,[1] Et, OMe, F, Cl, Br or CN) were characterised by elemental analysis (C, H and N) and by their IR carbonyl spectra (Table 1). The spectra are very similar to that of $[Rh_2(CO)_4(\mu\text{-}p\text{-}MeC_6H_4NNNC_6H_4Me\text{-}p)_2]$[12] but show small shifts to higher wavenumber, in ν(CO), as the electron-withdrawing capacity of the substituents X and X′ increases. In the complexes with asymmetric triazenide ligands, namely $[Rh_2(CO)_4(\mu\text{-}PhNNNC_6H_4X'\text{-}p)_2]$ (X′ = OMe or NO_2), two isomers are possible, *i.e.* head-to-tail (**A**) and head-to-head (**B**) (Scheme 1). Although their IR carbonyl spectra are

DOI: 10.1039/b002939o

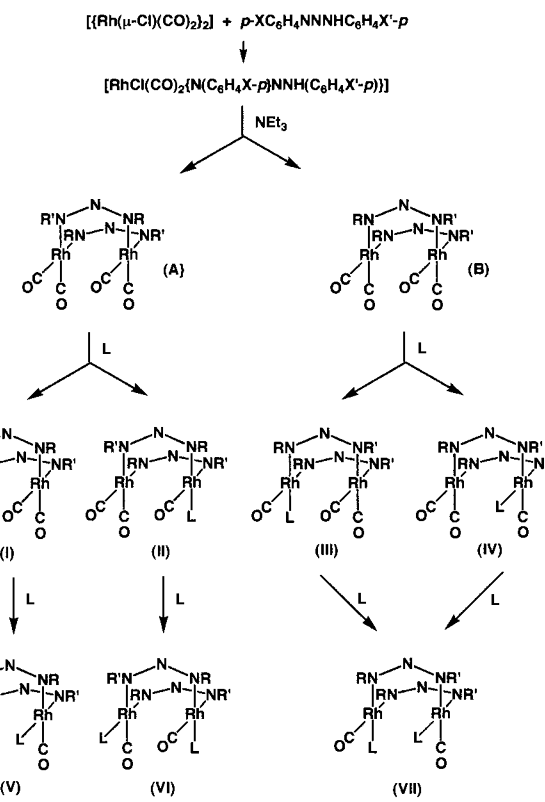

Scheme 1 R = C_6H_4X-*p*, R′ = C_6H_4X'-*p*, L = PPh_3.

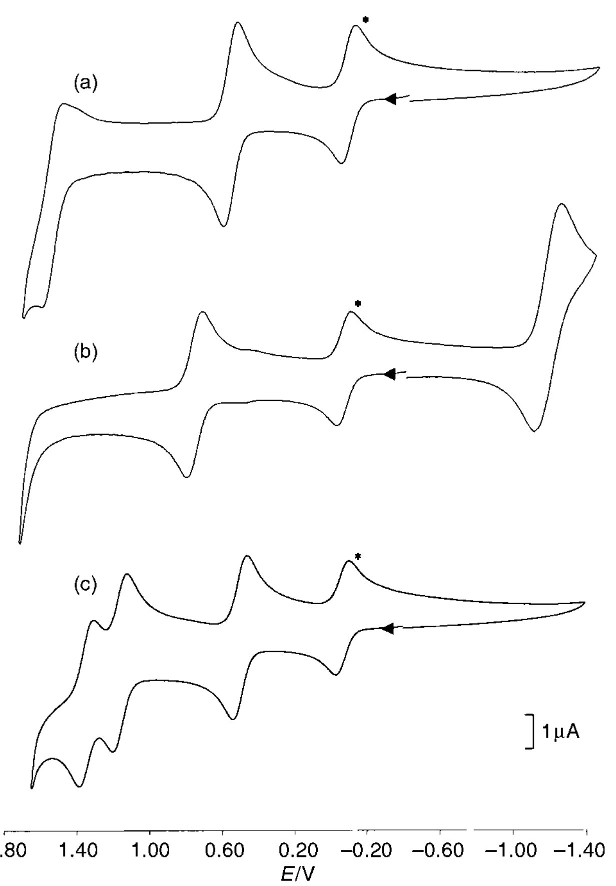

Fig. 1 The cyclic voltammograms of $[Rh_2(CO)_3(PPh_3)(\mu\text{-}p\text{-}XC_6H_4NNNC_6H_4X'\text{-}p)_2]$; (a) X = X′ = H, (b) X = H, X′ = NO_2, and (c) X = X′ = OMe, scanned from −0.4 to 1.65 to −1.4 to −0.4 V. In each case the wave marked with an asterisk (*) is due to the oxidation of $[Fe(\eta\text{-}C_5Me_5)_2]$, added as an internal potential standard.

indistinguishable, ^{31}P NMR spectroscopy clearly showed the formation of all possible derivatives when the two isomers were reacted with PPh_3.

The tetracarbonyl complexes undergo stepwise carbonyl substitution with PPh_3 to give $[Rh_2(CO)_{4-n}(PPh_3)_n(\mu\text{-}p\text{-}XC_6H_4NNNC_6H_4X'\text{-}p)_2]$ (*n* = 1 or 2). Previously, we have reported only the synthesis of the dicarbonyl $[Rh_2(CO)_2(PPh_3)_2(\mu\text{-}p\text{-}MeC_6H_4NNNC_6H_4Me\text{-}p)_2]$, it precipitating directly from the reaction between $[Rh_2(CO)_4(\mu\text{-}p\text{-}MeC_6H_4NNNC_6H_4Me\text{-}p)_2]$ and PPh_3 in *n*-hexane.[12] However, when the carbonyl substitution reactions were carried out in CH_2Cl_2, with the reactants in the appropriate proportions and with careful monitoring of the reaction by IR spectroscopy (the rate of carbonyl substitution is markedly dependent on X and X′), both the tri- and di-carbonyls were isolated as red crystalline solids. Again, the energies of the IR carbonyl bands depend on X and X′ (Table 1).

The PPh_3 complexes were also characterised by ^{31}P NMR spectroscopy (Table 1). The spectra are simple for the complexes in which X = X′, but provide evidence for the formation of isomers when X and X′ differ. Each of the tricarbonyls $[Rh_2(CO)_3(PPh_3)(\mu\text{-}p\text{-}XC_6H_4NNNC_6H_4X'\text{-}p)_2]$ (X = X′ = H, Me, Et, OMe, F, Cl, Br or CN) shows a single doublet resonance, in the range δ 39.8–40.4, with $J(^{31}P^{103}Rh)$ *ca.* 150 Hz. Likewise, each of the symmetrical dicarbonyls $[Rh_2(CO)_2(PPh_3)_2(\mu\text{-}p\text{-}XC_6H_4NNNC_6H_4X'\text{-}p)_2]$ (X = X′ = H or Et) gives only one doublet, consistent with the formation of only one isomer, *i.e.* that in which the two PPh_3 ligands, one on each metal atom, are *trans* disposed with respect to the Rh···Rh vector (as observed in the crystal structure of $[Rh_2(CO)_2(PPh_3)_2(\mu\text{-}p\text{-}MeC_6H_4NNNC_6H_4Me\text{-}p)_2]$).[4]

By contrast, the ^{31}P NMR spectra of $[Rh_2(CO)_{4-n}(PPh_3)_n(\mu\text{-}p\text{-}XC_6H_4NNNC_6H_4X'\text{-}p)_2]$ (X = H, X′ = OMe or NO_2, *n* = 1 or 2) show the presence of all possible isomers. As shown in Scheme 1, monosubstitution of the two forms of the asymmetrically bridged tetracarbonyls leads to four possible isomers, two (**I** and **II**) from the head-to-tail dimer **A** and two (**III** and **IV**) from the head-to-head isomer **B**. Accordingly, four doublets are observed, at δ 39.87, 39.99, 40.24 and 40.27 $\{J(^{31}P^{103}Rh) = 150, 151, 152$ and 151 Hz, respectively$\}$ for $[Rh_2(CO)_3(PPh_3)(\mu\text{-}PhNNNC_6H_4NO_2\text{-}p)_2]$ and at δ 40.22, 40.26, 40.29 and 40.35 $\{J(^{31}P^{103}Rh) = 152, 148, 150$ and 152 Hz respectively$\}$ for $[Rh_2(CO)_3(PPh_3)(\mu\text{-}PhNNNC_6H_4OMe\text{-}p)_2]$. Further substitution leads to three dicarbonyl isomers (**V** and **VI** from **I** and **II** respectively, and **VII** from both **III** and **IV**), and therefore three doublets $[J(^{31}P^{103}Rh) = 158$ Hz], at δ 39.70, 39.95 and 40.35 for $[Rh_2(CO)_2(PPh_3)_2(\mu\text{-}PhNNNC_6H_4NO_2\text{-}p)_2]$. Unfortunately, in no case could the various isomers be separated so that no definitive spectral assignment could be made.

Electrochemical studies

All of the dirhodium complexes $[Rh_2(CO)_{4-n}(PPh_3)_n(\mu\text{-}p\text{-}XC_6H_4NNNC_6H_4X'\text{-}p)_2]$ (*n* = 0–2) show at least one oxidation wave in the cyclic voltammogram (in the potential range 1.5 to −1.5 V, in CH_2Cl_2, at a Pt electrode); the redox potential of this, and subsequent electron transfer reactions (Table 1), depends on the substituents X and X′ as described below. The cyclic voltammograms of $[Rh_2(CO)_3(PPh_3)(\mu\text{-}p\text{-}XC_6H_4NNNC_6H_4X'\text{-}p)_2]$ (X = X′ = H; X = H, X′ = NO_2; X = X′ = OMe) are shown as representative examples in Fig. 1(a)–(c), respectively.

For all of the complexes $[Rh_2(CO)_{4-n}(PPh_3)_n(\mu\text{-}p\text{-}XC_6H_4NNNC_6H_4X'\text{-}p)_2]$ (except X = X′ = CN) the first oxidation wave is fully reversible and corresponds to the formation of the monocation $[Rh_2(CO)_{4-n}(PPh_3)_n(\mu\text{-}p\text{-}XC_6H_4NNNC_6H_4X'\text{-}p)_2]^+$, as found for the archetypal compounds $[Rh_2(CO)_{4-n}(PPh_3)_n(\mu\text{-}p\text{-}MeC_6H_4NNNC_6H_4Me\text{-}p)_2]$ (*n* = 0 and 2).[1] A second oxidation wave, corresponding to the formation of $[Rh_2(CO)_{4-n}(PPh_3)_n(\mu\text{-}p\text{-}XC_6H_4NNNC_6H_4X'\text{-}p)_2]^{2+}$, is also usually observed though in some cases it is irreversible, implying instability of the dication. For some of the tetracarbonyls

Table 1 Analytical, electrochemical and spectroscopic data for $[Rh_2(CO)_{4-n}(PPh_3)_n(\mu\text{-}p\text{-}XC_6H_4NNNC_6H_4X'\text{-}p)_2]$

				Analysis (%)[a]					
n	X	X′	Yield (%)	C	H	N	$E°$/V[b]	ν(CO)/cm^{-1} [c]	^{31}P NMR[d]
0	H	H	51	47.7(47.4)	2.8(2.8)	11.9(11.8)	0.88, 1.6(I)	2090vs, 2062m, 2026	—
1	H	H	48	57.5(57.2)	4.0(3.7)	8.9(8.9)	0.56, 1.56(I)[e]	2064, 2002, 1986m	40.28(151)
2	H	H	88	63.4(63.2)	4.5(4.3)	6.9(7.1)	0.22, 1.43	1980, 1966	40.04(157)
0	Me	Me[f]					0.83, 1.42	2089vs, 2061m, 2024	—
1	Me	Me	32	58.8(58.8)	4.1(4.3)	8.5(8.4)	0.50, 1.37[e]	2062, 2000, 1985m	40.37(151)
2	Me	Me[f]					0.18, 1.28, 1.57	1978, 1963	—
0	Et	Et	80	52.6(52.6)	4.6(4.4)	10.2(10.2)	0.82	2088vs, 2060m, 2023	—
1	Et	Et	70	60.2(60.2)	5.0(4.9)	7.8(8.0)	0.51, 1.40[e]	2062, 2000, 1984m	40.27(151)
2	Et	Et	80	65.5(65.1)	5.8(5.2)	6.5(6.5)	0.17, 1.29, 1.57	1978, 1965	39.98(157)
0	OMe	OMe	60	46.5(46.3)	3.6(3.4)	9.7(10.1)	0.80, 1.20, 1.37	2088vs, 2059m, 2022	—
1	OMe	OMe	93	55.3(55.2)	3.9(4.1)	7.7(7.9)	0.49, 1.14, 1.34	2060, 1998, 1984m	40.36(152)
2	OMe	OMe	63	61.4(61.0)	4.5(4.5)	6.4(6.5)	0.18, 1.07, 1.26	1976, 1965	—
0	CN	CN	73	47.4(47.4)	1.7(2.0)	16.9(17.3)	1.09(I), −1.37(I)[g]	2100vs, 2073m, 2039	—
1	CN	CN	65	56.9(56.3)	3.1(3.0)	13.4(13.4)	0.81	2074, 2015, 1995m	39.79(151)
2	CN	CN	33	62.0(62.0)	3.9(3.6)	9.5(11.0)	0.55	1990, 1977	—
0	H	OMe	84	47.2(46.8)	2.9(3.1)	11.5(10.9)	0.84, 1.37	2089vs, 2061m, 2024	—
1	H	OMe	57	56.5(56.2)	4.1(3.9)	8.3(8.4)	0.51, 1.30, 1.48	2063, 2000, 1985m	[h]
2	H	OMe	75	61.5(62.1)	4.5(4.4)	6.0(6.8)	0.21, 1.22, 1.41	1979, 1965	—
0	H	NO_2	44	42.0(42.0)	3.0(2.3)	14.1(14.0)	0.97	2096vs, 2069m, 2034	—
1	H	NO_2	88	52.3(52.2)	3.1(3.2)	10.7(10.8)	0.71, −1.10[g]	2070, 2010, 1990m	[h]
2	H	NO_2	70	60.6(60.3)[i]	4.5(4.6)	8.5(8.3)	0.42, 1.61, −1.22[g]	1987, 1974	[h]
0	F	F	86	43.4(43.0)	2.1(2.1)	10.9(10.7)	0.91, 1.64(I)	2092vs, 2065m, 2029	—
1	F	F	66	53.4(53.2)	3.1(3.1)	7.9(8.3)	0.62, 1.55(I)	2066, 2004, 1988m	40.27(151)
2	F	F	66	59.3(59.5)	3.6(3.7)	6.6(6.7)	0.32, 1.48	1982, 1968	40.18(157)
0	Cl	Cl	31	40.1(39.7)	1.7(1.9)	9.7(9.9)	0.95	2094vs, 2066m, 2031	—
1	Cl	Cl	58	49.9(49.9)	2.9(2.9)	7.0(7.8)	0.65	2068, 2007, 1990m	40.23(151)
2	Cl	Cl	60	57.0(56.6)	3.9(3.5)	5.7(6.4)	0.37, 1.52	1984, 1970	—
0	Br	Br	53	33.4(32.8)	1.5(1.6)	8.2(8.2)	0.95	2094vs, 2067m, 2031	—
1	Br	Br	63	42.5(42.9)	2.2(2.5)	5.8(6.7)	0.67, 1.64(I)	2068, 2007, 1991m	40.28(150)
2	Br	Br	55	51.4(51.7)[i]	3.7(3.8)	5.4(5.3)	0.38, 1.54	1984, 1971	—

[a] Calculated values in parentheses. [b] $E°'$ for reversible one-electron oxidation wave unless otherwise stated. The oxidation peak potential, $(E_p)_{ox}$, at a scan rate of 200 mV s^{-1} is given for an irreversible (I) wave. Unless stated otherwise, potentials were calibrated *vs.* the following internal standards: tetracarbonyls *vs.* the couple $[Fe(\eta\text{-}C_5H_5)_2]^+/[Fe(\eta\text{-}C_5H_5)_2]$ (0.47 V); tricarbonyls *vs.* the couple $[Fe(\eta\text{-}C_5Me_5)_2]^+/[Fe(\eta\text{-}C_5Me_5)_2]$ (−0.08 V); dicarbonyls *vs.* the couple $[Fe(\eta\text{-}C_5H_4COMe)_2]^+/[Fe(\eta\text{-}C_5H_4COMe)_2]$ (0.97 V). [c] In CH_2Cl_2; strong (s) absorptions unless otherwise stated, m = medium, vs = very strong. [d] Spectra in CD_2Cl_2; chemical shift in ppm with $J(^{31}P^{103}Rh)$ in Hz in parentheses. [e] Potentials calibrated *vs.* the couple $[Fe(\eta\text{-}C_5H_4COMe)_2]^+/[Fe(\eta\text{-}C_5H_4COMe)_2]$. [f] Data from ref. 1. [g] Reduction wave, see text. [h] Several isomers present, see text. [i] Sample analysed as a 1.0 *n*-hexane solvate.

(X = X′ = Et, F, Cl or Br; X = H, X′ = NO_2) and for all of the *p*-cyano complexes the second oxidation wave was not observed; it is presumed to occur at a potential obscured by the base electrolyte background curve.

For $[Rh_2(CO)_2(PPh_3)_2(\mu\text{-}p\text{-}XC_6H_4NNNC_6H_4X\text{-}p)_2]$ (X = X′ = Me or Et) and for all of the complexes in which the bridging ligands bear a *p*-OMe substituent (*i.e.* X = OMe, X′ = H or OMe, *n* = 0–2) a third reversible wave corresponding to the formation of $[Rh_2(CO)_{4-n}(PPh_3)_n(\mu\text{-}p\text{-}XC_6H_4NNNC_6H_4X\text{-}p)_2]^{3+}$ was detected. Finally, in the case of $[Rh_2(CO)_{4-n}(PPh_3)_n(\mu\text{-}PhNNNC_6H_4NO_2\text{-}p)_2]$ a *reduction* wave was observed. Though ill-defined for the tetracarbonyl (*n* = 0), the waves for $[Rh_2(CO)_3(PPh_3)(\mu\text{-}PhNNNC_6H_4NO_2\text{-}p)_2]$ [Fig. 1(b)] and $[Rh_2(CO)_2(PPh_3)_2(\mu\text{-}PhNNNC_6H_4NO_2\text{-}p)_2]$, at −1.10 and −1.22 V, respectively, were reversible and approximately twice the height of those for the corresponding oxidation waves. Given the well-known reduction of nitrobenzene to its anion radical $[C_6H_5NO_2]^-$,[13] and the small shift in potential (*ca.* 120 mV) as *n* is increased from 1 to 2 (*cf.* shifts of *ca.* 300 mV on oxidation) these reductions may be associated with electron addition to the *p*-$NO_2C_6H_4$ groups.

For all three series of complexes (*n* = 0–2) the oxidation potentials depend significantly on the aryl substituents X and X′. {Potentials, measured to the nearest 10 mV, have been internally calibrated using $[Fe(\eta\text{-}C_5H_5)_2]$ (for *n* = 0), $[Fe(\eta\text{-}C_5Me_5)_2]$ (for *n* = 1) or $[Fe(\eta\text{-}C_5H_4COMe)_2]$ (for *n* = 2); each calibrant was chosen so that its oxidation wave did not obscure those of the compound under study.} Those for the first oxidation process cover ranges of *ca.* 250, 320 and 370 mV for *n* = 0–2 respectively. Taken with the effect of replacing CO by PPh_3 (for a given substituent, each increment in *n* leads to a shift in $E°'$ of *ca.* 300 mV to more negative potentials), the potential for the $[Rh_2]^{2+}$–$[Rh_2]^{3+}$ couple can be tuned systematically over a range of *ca.* 800 mV (*i.e.* from 0.17 to 0.97 V). {The range is increased to *ca.* 900 mV if the peak potential, $(E_p)_{ox}$, for the irreversible oxidation wave of $[Rh_2(CO)_4(\mu\text{-}p\text{-}NCC_6H_4NNNC_6H_4CN\text{-}p)_2]$ is included.}

There is a general dependence of the potentials $E°'$ on X and X′ such that electron-donating substituents facilitate oxidation. However, more quantitative relationships can be explored[14] by considering Hammett substituent constants. An early study by Kadish and co-workers showed[15] linear correlations between such constants and $E°'$ for both the oxidation and reduction of the carboxylate complexes $[Rh_2(\mu\text{-}O_2CR)_4]$ and Ren has more recently reviewed[5] his extensive studies of the effects of substituent on the redox behaviour of $[M_2(\mu\text{-}L)_4]$ (L = diarylformamidinate). In these 'lantern-like' (or 'paddle-wheel') complexes all of the various redox processes show a linear correlation between $E°'$ and Hammett constants. For example, $[Rh_2(\mu\text{-}L)_4]$ undergoes three successive one-electron oxidations with essentially identical reaction constants of 96, 98 and 97 mV, respectively.

Our results, with dirhodium complexes having a rather less rigid di-bridged structure, are somewhat different. Plots of $E°_1{}'$ (the potential for the first, reversible, one-electron oxidation) *vs.* $4\sigma_p$ (given the four substituents, two on each bridging ligand) are linear in all cases (correlation coefficients, 0.97, 0.98 and 0.96 for *n* = 0, 1 and 2, respectively) (Fig. 2) with reaction constants 71, 91 and 108 mV. However, plots of $E°_2{}'$ (the potential for the second one-electron oxidation step) *vs.* $4\sigma_p$ for

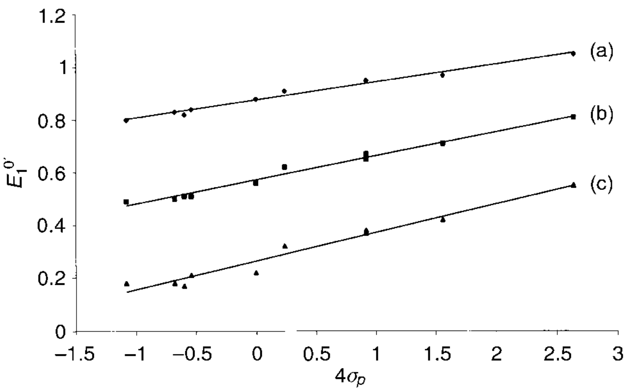

Fig. 2 Plots of $E^{\circ}{}_1{}'$ *vs.* $4\sigma_p$ for (a) $[Rh_2(CO)_4(\mu\text{-}p\text{-}XC_6H_4NNNC_6H_4X'\text{-}p)_2]$, (b) $[Rh_2(CO)_3(PPh_3)(\mu\text{-}p\text{-}XC_6H_4NNNC_6H_4X'\text{-}p)_2]$, and (c) $[Rh_2(CO)_2(PPh_3)_2(\mu\text{-}p\text{-}XC_6H_4NNNC_6H_4X'\text{-}p)_2]$.

$[Rh_2(CO)_{4-n}(PPh_3)_n(\mu\text{-}p\text{-}XC_6H_4NNNC_6H_4X'\text{-}p)_2]$ show poorer correlations of 0.79, 0.73 and 0.90 for $n = 0$–2 respectively. (Somewhat better values, of 0.93, 0.82 and 0.90, were obtained by including estimates of $E^{\circ}{}'$ for those species which show irreversible oxidation waves.) The reason for the difference between $[Rh_2(CO)_{4-n}(PPh_3)_n(\mu\text{-}p\text{-}XC_6H_4NNNC_6H_4X'\text{-}p)_2]$ and $[Rh_2(\mu\text{-}L)_4]$ (L = diarylformamidinate) is unclear but may be related to structural distortions on oxidation. X-Ray crystallographic studies on $[Rh_2\{\mu\text{-}XC_6H_4NC(H)NC_6H_4X\}_2\}_4]$ (X = H,[16] *p*-Me[17] or *m*-OMe[8]) and $[Rh_2\{\mu\text{-}RNC(H)NR\}_2\}_4]$ (R = $C_6H_3Cl_2$-3,5),[8] with substituents having a range of Hammett constants, have a rigid framework with almost invariant geometry (*e.g.* very similar Rh–Rh and Rh–N distances) indicating "the absence of substituent perturbation on the geometry of the dinuclear core".[8] By contrast, the carbonyl complexes are more flexible so that oxidation of $[Rh_2(CO)_2(PPh_3)_2(\mu\text{-}p\text{-}MeC_6H_4NNNC_6H_4Me\text{-}p)_2]$ and the diphenylacetamidinate analogues $[Rh_2(CO)_2LL'\{\mu\text{-}PhNC(Me)NPh\}_2]$ {L, L′ = PPh_3 or $P(OPh)_3$}[4] leads to a marked distortion; the interplane and staggering angles between the two Rh^I square planes are reduced on oxidation (as the rhodium–rhodium distance decreases). Such angular distortions are likely to increase as the Rh–Rh distance further shortens on the loss of the second electron from the Rh_2 σ* orbital, perhaps irregularly affecting $E^{\circ}{}_2{}'$ and hence leading to the poorer observed correlation with σ_p.

Experimental

The preparation, purification and reactions of the complexes described were carried out under an atmosphere of dry dinitrogen using dried, distilled and deoxygenated solvents; reactions were monitored by IR spectroscopy where necessary. The compound $[\{Rh(\mu\text{-}Cl)(CO)_2\}_2]$[18] and the triazenes RNNNHR′[19] were prepared by published methods. The tetracarbonyls $[Rh_2(CO)_4(\mu\text{-}p\text{-}XC_6H_4NNNC_6H_4X'\text{-}p)_2]$ (X = X′ = H or Et; X = H, X′ = OMe) were prepared by the method used for $[Rh_2(CO)_4(\mu\text{-}p\text{-}MeC_6H_4NNNC_6H_4Me\text{-}p)_2]$.[1] Where the complexes $[Rh_2(CO)_{4-n}(PPh_3)_n(\mu\text{-}p\text{-}XC_6H_4NNNC_6H_4X'\text{-}p)_2]$ ($n = 1$ or 2) were purified using a mixture of two solvents, the impure solid was dissolved in the more polar solvent, the resulting solution was filtered and then treated with the second solvent, and the mixture reduced in volume *in vacuo* to induce precipitation. IR and ^{31}P NMR spectra were recorded on Nicolet 5ZDX FT and JEOL λ300 spectrometers, respectively. Electrochemical studies were carried out using an EG&G model 273A potentiostat (computer-controlled using EG&G model 270 Research Electrochemistry software) in conjunction with a three-electrode cell. For cyclic voltammetry the auxiliary electrode was a platinum wire and the working electrode a platinum disc. The reference was an aqueous saturated calomel electrode (SCE) separated from the test solution by a fine-porosity frit and an agar bridge saturated with KCl. Solutions in CH_2Cl_2 were 0.1×10^{-3} mol dm^{-3} or 5×10^{-4} mol dm^{-3} in the test compound and 0.1 mol dm^{-3} in $[NBu_4][PF_6]$ as the supporting electrolyte. Under the conditions used, $E^{\circ}{}'$ for the one-electron oxidations of $[Fe(\eta\text{-}C_5H_5)_2]$, $[Fe(\eta\text{-}C_5Me_5)_2]$ or $[Fe(\eta\text{-}C_5H_4COMe)_2]$, added to the test solutions as internal calibrants, are 0.47, −0.08 and 0.97 V, respectively. Microanalyses were carried out by the staff of the Microanalytical Service of the School of Chemistry, University of Bristol.

Syntheses

$[Rh_2(CO)_4(\mu\text{-}p\text{-}FC_6H_4NNNC_6H_4F\text{-}p)_2]$. A mixture of $[\{Rh(\mu\text{-}Cl)(CO)_2\}_2]$ (0.10 g, 0.26 mmol) and *p*-$FC_6H_4NNNHC_6H_4F$-*p* (0.126 g, 0.54 mmol) in CH_2Cl_2 (10 cm^3) was stirred for 10 min and then NEt_3 (0.084 cm^3, 0.60 mmol) was added. The red solution was evaporated to low volume (*ca.* 5 cm^3) and then placed on an alumina–diethyl ether chromatography column. Elution with diethyl ether gave an orange band which was collected. *n*-Hexane (20 cm^3) was added to the red eluate and the mixture evaporated to low volume and then cooled to −20 °C to give red crystals, yield 0.183 g (86%).

The complexes $[Rh_2(CO)_4(\mu\text{-}p\text{-}XC_6H_4NNNC_6H_4X'\text{-}p)_2]$ (X = X′ = Cl or Br) were prepared similarly as red crystals. The following modifications were made in order to synthesise $[Rh_2(CO)_4(\mu\text{-}p\text{-}XC_6H_4NNNC_6H_4X'\text{-}p)_2]$: X = X′ = CN, reaction time 1 h, chromatography on Florisil–CH_2Cl_2, elution with CH_2Cl_2, eluate evaporated after addition of *n*-hexane; X = X′ = OMe, reaction time 3 min, chromatography on alumina–*n*-hexane, elution with diethyl ether, evaporation of eluate to low volume and cooling to −20 °C; X = H, X′ = NO_2, reaction time 20 min, chromatography on Florisil–*n*-hexane, elution with CH_2Cl_2–*n*-hexane (1 : 1).

$[Rh_2(CO)_3(PPh_3)(\mu\text{-}PhNNNPh)_2]$. Solid PPh_3 (0.118 g, 0.45 mmol) was added to a stirred solution of $[Rh_2(CO)_4(\mu\text{-}PhNNNPh)_2]$ (0.30 g, 0.42 mmol) in CH_2Cl_2 (20 cm^3). After 10 min the red solution was evaporated to low volume (*ca.* 5 cm^3) and then placed on a silica–*n*-hexane chromatography column. Elution with CH_2Cl_2–*n*-hexane (3 : 10) gave a red band which was collected, evaporated to low volume (*ca.* 5 cm^3) and then cooled to −20 °C to give red crystals, yield 0.19 g (48%).

The complexes $[Rh_2(CO)_3(PPh_3)(\mu\text{-}p\text{-}XC_6H_4NNNC_6H_4X'\text{-}p)_2]$ (X = X′ = Me or Et; X = H, X′ = OMe) were prepared similarly but without the need for chromatography. The reaction mixture was filtered, *n*-hexane was added, and the volume of the solvent was reduced to give the solid product.

$[Rh_2(CO)_3(PPh_3)(\mu\text{-}p\text{-}FC_6H_4NNNC_6H_4F\text{-}p)_2]$. Solid PPh_3 (0.061 g, 0.23 mmol) was added to a stirred solution of $[Rh_2(CO)_4(\mu\text{-}p\text{-}FC_6H_4NNNC_6H_4F\text{-}p)_2]$ (0.183 g, 0.23 mmol) in CH_2Cl_2 (10 cm^3). After 10 min, *n*-hexane (20 cm^3) was added, and then the mixture was evaporated to low volume and cooled to −20 °C to give red crystals, yield 0.156 g (66%).

The complexes $[Rh_2(CO)_3(PPh_3)(\mu\text{-}p\text{-}XC_6H_4NNNC_6H_4X'\text{-}p)_2]$ (X = X′ = MeO, CN, Cl or Br) were prepared similarly; in the case of X = X′ = Br the complex was purified using CH_2Cl_2–isopropanol.

$[Rh_2(CO)_3(PPh_3)(\mu\text{-}PhNNNC_6H_4NO_2\text{-}p)_2]$. Solid PPh_3 (0.065 g, 0.25 mmol) was added to a stirred solution of $[Rh_2(CO)_4(\mu\text{-}PhNNNC_6H_4NO_2\text{-}p)_2]$ (0.20 g, 0.25 mmol) in CH_2Cl_2 (20 cm^3). After 20 min the mixture was evaporated to low volume (*ca.* 5 cm^3) and placed on an alumina–CH_2Cl_2 chromatography column. Elution with CH_2Cl_2 gave a red band which was collected and then evaporated to dryness to give a red solid, yield 0.23 g (88%).

$[Rh_2(CO)_2(PPh_3)_2(\mu\text{-}PhNNNPh)_2]$. Solid PPh_3 (0.354 g, 1.35 mmol) was added to a stirred solution of $[Rh_2(CO)_4$-

(μ-PhNNNPh)$_2$] (0.16 g, 0.23 mmol) in CH_2Cl_2 (20 cm^3). After 1 h the red solution was filtered, *n*-hexane was added, and the mixture was evaporated to low volume to give a red solid which was purified using CH_2Cl_2–*n*-hexane to give red crystals, yield 0.24 g (88%).

The complexes [$Rh_2(CO)_2(PPh_3)_2(\mu$-*p*-$XC_6H_4NNNC_6H_4X'$-*p*)$_2$] (X = X′ = F or OMe) were prepared similarly. The complex [$Rh_2(CO)_2(PPh_3)_2(\mu$-$PhNNNC_6H_4NO_2$-*p*)$_2$] was isolated as a dark brown solid after addition of *n*-hexane to the filtered reaction mixture (reaction time 2 h), reduction of the solution volume *in vacuo* and storage at −20 °C.

[$Rh_2(CO)_2(PPh_3)_2(\mu$-*p*-$EtC_6H_4NNNC_6H_4Et$-*p*)$_2$]. Solid PPh_3 (0.272 g, 1.04 mmol) was added to a stirred solution of [$Rh_2(CO)_4(\mu$-*p*-$EtC_6H_4NNNC_6H_4Et$-*p*)$_2$] (0.43 g, 0.52 mmol) in *n*-hexane (100 cm^3). After 24 h the red precipitate was removed by filtration and then purified using CH_2Cl_2–*n*-hexane to give red microcrystals, yield 0.53 g (80%).

The complexes [$Rh_2(CO)_2(PPh_3)_2(\mu$-*p*-$XC_6H_4NNNC_6H_4X'$-*p*)$_2$] (X = X′ = Cl or Br; X = H, X′ = OMe) were prepared similarly.

[$Rh_2(CO)_2(PPh_3)_2(\mu$-*p*-$NCC_6H_4NNNC_6H_4CN$-*p*)$_2$]. A mixture of [{$Rh(\mu$-$Cl)(CO)_2$}$_2$] (0.126 g, 0.32 mmol) and *p*-$NCC_6H_4NNNHC_6H_4CN$-*p* (0.161 g, 0.65 mmol) in CH_2Cl_2 (15 cm^3) was stirred for 3.5 h and then NEt_3 (0.115 cm^3, 0.80 mmol) was added. After 20 min, PPh_3 (0.168 g, 0.64 mmol) was added and after stirring for a further 90 min the mixture was evaporated to dryness. The residue was extracted into toluene (10 cm^3) and then *n*-hexane (20 cm^3) was added to the filtered extract. The mixture was evaporated to low volume to give a red precipitate which was purified using CH_2Cl_2–*n*-hexane to give red–brown crystals, yield 0.135 g (33%).

Acknowledgements

We thank the Royal Thai Government for a Postgraduate Scholarship (to P. K.).

References

1 N. G. Connelly, G. Garcia, M. Gilbert and J. S. Stirling, *J. Chem. Soc., Dalton Trans.*, 1987, 1403.

2 T. Brauns, C. Carriedo, J. S. Cockayne, N. G. Connelly, G. Garcia Herbosa and A. G. Orpen, *J. Chem. Soc., Dalton Trans.*, 1989, 2049.

3 N. G. Connelly, T. Einig, G. Garcia Herbosa, P. M. Hopkins, C. Mealli, A. G. Orpen, G. M. Rosair and F. Viguri, *J. Chem. Soc., Dalton Trans.*, 1994, 2025; N. G. Connelly, P. M. Hopkins, A. G. Orpen, G. M. Rosair and F. Viguri, *J. Chem. Soc., Dalton Trans.*, 1992, 2907; M. Bardaji, N. C. Brown, A. Christofides and N. G. Connelly, *J. Organomet. Chem.*, 1994, **474**, C24.

4 D. C. Boyd, N. G. Connelly, G. Garcia Herbosa, M. G. Hill, K. R. Mann, C. Mealli, A. G. Orpen, K. E. Richardson and P. H. Rieger, *Inorg. Chem.*, 1994, **33**, 960.

5 T. Ren, *Coord. Chem. Rev.*, 1998, **175**, 43.

6 C. Lin, J. D. Protasiewicz and T. Ren, *Inorg. Chem.*, 1996, **35**, 7455.

7 C. Lin, J. D. Protasiewicz, E. T. Smith and T. Ren, *Inorg. Chem.*, 1996, **35**, 6422.

8 T. Ren, C. Lin, E. J. Valente and J. D. Zubkowski, *Inorg. Chim. Acta*, 2000, **297**, 283.

9 C. Lin, T. Ren, E. J. Valente and J. D. Zubkowski, *J. Chem. Soc., Dalton Trans.*, 1998, 571.

10 C. Lin, T. Ren, E. J. Valente, J. D. Zubkowski and E. T. Smith, *Chem. Lett.*, 1997, 753.

11 C. Hansch, A. Leo and R. W. Taft, *Chem. Rev.*, 1991, **91**, 165.

12 N. G. Connelly, H. Daykin and Z. Demidowicz, *J. Chem. Soc., Dalton Trans.*, 1978, 1532.

13 See, for example: A. H. Maki and D. H. Geske, *J. Am. Chem. Soc.*, 1961, **83**, 1852; S. Vijayalakshamma and R. S. Subrahmanya, *J. Electroanal. Chem. Interfacial Electrochem.*, 1969, **23**, 99.

14 C. J. Pickett, in *Comprehensive Coordination Chemistry*, eds. G. Wilkinson, R. D. Gillard and J. A. McCleverty, Pergamon Press, Oxford, 1987, vol. 1, ch. 8.3, p. 497.

15 K. Das, K. M. Kadish and J. L. Bear, *Inorg. Chem.*, 1978, **17**, 930.

16 J. L. Bear, C.-L. Yao, R. S. Lifsey, J. D. Korp and K. M. Kadish, *Inorg. Chem.*, 1991, **30**, 336.

17 P. Piraino, G. Bruno, S. Lo Schiavo, F. Laschi and P. Zanello, *Inorg. Chem.*, 1987, **26**, 2205.

18 J. A. McCleverty and G. Wilkinson, *Inorg. Synth.*, 1990, **28**, 84.

19 W. W. Hartman and J. B. Dickey, *Org. Synth.*, 1943, **Coll. Vol. II**, 163.